Finite Element Method for Finite-Size Scaling in Quantum Mechanics

Winton Moy, Marcelo A. Carignano, and Sabre Kais*

Department of Chemistry, Purdue University, West Lafayette, Indiana 47907

Received: January 14, 2008; Revised Manuscript Received: March 28, 2008

We combined the finite-size scaling method with the finite element method to provide a systematic procedure for obtaining quantum critical parameters for a quantum system. We present results for the Yukawa potential solved with the finite element approach. The finite-size scaling approach was then used to find the critical parameters of the system. The critical values λ_c, α, and ν were found to be 0.83990345, 2.0002, and 1.002, respectively, for $l = 0$. These results compare well with the theoretically exact values for α and ν and with the best numerical estimations for λ_c. The finite element method is general and can be extended to larger systems.

I. Introduction

Phase transitions are associated with singularities of the free energy. These singularities occur only in the thermodynamic limit[1,2] where the dimension of the system approaches infinity. However, calculations are done only on finite systems. A finite-size scaling (FSS) approach is needed in order to exptrapolate results from finite systems to the thermodynamic limit.[3] FSS is not only a formal way to understand the asymptotic behavior of a system when the size tends to infinity but a theory that also gives us numerical methods[4–11] capable of obtaining accurate results for infinite systems by studying the corresponding small systems.

Recently, we have applied the FSS theory to quantum systems.[12–21] In this approach, the finite size corresponds not to the spatial dimension but to the number of elements in a complete basis set used to expand the exact eigenfunction of a given Hamiltonian. This method is efficient and very accurate for estimating the critical screening length for one-electron screened Coulomb potentials,[21] the critical nuclear charges for two-electron atoms[12,16] (which was found to be in complete agreement with previous calculations)[22,23] and three-electron atoms,[13] critical conditions for stable dipole-bound anions,[24] critical conditions for stable quadrupole-bound anions,[25] simple diatomic molecules,[26] three-body Coulomb systems with charges (Q, q, Q) and masses (M, m, M),[27] the criticality of atomic Shannon information entropy,[28] and crossover phenomena and resonances in quantum systems.[29]

All of our previous FSS calculations are done based on expanding the wave function in a Hyllarass-type basis set or, more generally, in a Slater-type basis set. Recently, we were able to apply Gaussian-type basis functions to achieve the same results.[30]

For this paper, we combine the finite element method (FEM) with FSS to investigate the critical behavior of a quantum system. FEM is used to solve the corresponding Schrödinger equation and provide the needed inputs for the FSS method, namely, the ground-state energy and average potential energy as a function of the number of elements used in the solution. We will show how to use the FEM to perform a FSS analysis in order to study the criticality of quantum mechanical problems.

* To whom correspondence should be addressed. E-mail: kais@purdue.edu.

The FEM framework was first developed by Hrenikoff and Courant.[31,32] The formal presentation of the finite element method is attributed to Argyris and Kelsey[33] and also Turner, Clough, Martin, and Topp.[34] The use of the FEM was originally developed as a numerical technique for model problems in engineering and physics. For an overview of the finite element method and its development, a treatise of this area is given by Owen and Hinton.[35] The versatility of finite elements has led to applications for quantum mechanical problems. A comparison of the finite element method and the spectral method has been done for a two-dimensional bound state problem.[36] Calculations for atomic systems,[37–41] molecules,[42] atoms in a strong magnetic field,[38,43] hyperfine structure[44] of atoms, and molecules in a time-dependent external field[45,46] are just a few examples of the versatility of the FEM in quantum mechanical problems today.

In the next two sections, we outline the use of finite elements to solve for the Yukawa potential and the application of the finite element method with finite-size scaling. The last section contains the discussion of our results.

II. The Finite Element Method

The FEM is a numerical technique that gives approximate solutions to differential equations. In the case of quantum mechanics, the differential equation is formulated as a boundary value problem. For our purposes, we are interested in solving the time-independent Shrödinger equation with finite elements

$$H\Psi = E\Psi \tag{1}$$

The procedure for FEM to solve for differential equations can be found in many textbooks in engineering.[47,48] For more specific applications of finite elements to quantum mechanics, Ram-Mohan's book[49] gives an excellent introduction to this area. The general procedure for solving differential equations with FEM is given in the following steps: (1) discretization of the domain space into a finite number of n subdomains, for example, line segments for a one-dimensional problem; (2) for any nth element, we isolate it and specify its properties such as length, area, or volume; (3) the behavior of the solution within the nth element is approximated with shape functions; the contribution for the nth element is represented as a local matrix; (4) the individual local matrices are assembled together to form the global matrices H and S, which results in a generalized real-symmetric eigenvalue problem

10.1021/jp800346z CCC: $40.75
Published on Web 05/21/2008

$$H|\psi\rangle = ES|\psi\rangle \quad (2)$$

and (5) The generalized real-symmetric eigenvalue problem is solved with standard numerical analysis algorithms.

A didactic presentation of FEM applied to the hydrogen atom was published by Ram-Mohan.[38] Here, we outline the FEM applied to the short-range Yukawa potential

$$\left[-\frac{\hbar^2}{2m}\nabla^2 + \frac{l(l+1)}{r^2} - \frac{e^2 e^{-r/\lambda}}{r}\right]\psi(r) = E\psi(r) \quad (3)$$

where λ is the screening length and l is the angular quantum number. Using the Bohr radius a_0 as a unit length and rescaling the energy by the Rydberg unit $R_0 = \hbar^2/2ma_0^2 = e^2/2a_0$, the equation reads

$$\left[-\frac{d^2}{dr^2} - \frac{2}{r}\frac{d}{dr} + \frac{l(l+1)}{r^2} - \frac{2\lambda e^{-r}}{r}\right]\psi(r) = \epsilon\psi(r) \quad (4)$$

with $\epsilon = E\lambda^2/R_0$ used to represent the reduced energy. Equation 4 will be solved using FEM.

In order to apply the FEM, eq 4 needs to be expressed as a variational problem. This is achieved by multiplying with ψ^* (complex conjugate wave function) and integrating over the radial coordinate r from 0 to ∞. After an integration by parts, we obtain

$$\int_0^\infty [r^2\psi^{*'}(r)\psi'(r) + (l(l+1) - 2\lambda r e^{-r})\psi^*(r)\psi(r)]dr = \epsilon\int_0^\infty r^2\psi^*(r)\psi(r)dr \quad (5)$$

Equation 4 can be obtained as an extremus of eq 5 with respect to a variation on $\psi^*(r)$.

At this point, the standard approach to study bounded states is to introduce a cutoff r_c for the radial coordinate. For r_c sufficiently large, the error introduced by the cutoff is negligible. However, for our purpose of understanding the localization−delocalization critical condition, the use of a distance cutoff leads to inaccurate results. To overcome this problem, we define region A as the interval $[0, r_c]$ and region B as the infinite interval $[r_c,\infty)$. Region A is divided into N elements of equal length d_h. Region B will be treated as a single infinite element (see below). Element n in region A is defined as the segment $[r_{n-1}, r_n]$, with $r_n = nd_h$. Within element n, the radial coordinate is mapped to a local coordinate $x \in [-1, 1]$.

The wave function $\psi_n(x)$ in the nth element is expressed in terms of local shape functions, which, for our calculations, are Hermite interpolation polynomials with two nodes (left and right border of the elements) and three degrees of freedom. This choice ensures the continuity of the wave function and its first two derivatives. Then, in the nth element, the wave function is

$$\psi_n(x) = \sum_{\alpha=1}^{2}\left[\phi_\alpha(x)\psi_n^\alpha + \bar{\phi}_\alpha(x)\psi_n'^\alpha + \bar{\bar{\phi}}_\alpha(x)\psi_n''^\alpha\right] \quad (6)$$

with α indicating the nodal index of the element; $\alpha = 1$ for the left and $\alpha = 2$ for the right border of the element. The functions $\phi_\alpha(x)$, $\bar{\phi}_\alpha(x)$, and $\bar{\bar{\phi}}_\alpha(x)$ are the (fifth-degree) Hermite interpolation polynomials, which are described in ref 50. Then, ψ_n^α, $\psi_n'^\alpha$, and $\psi_n''^\alpha$ are the undetermined values of the wave function and its first and second derivative on the nodal points.

Using the local wave function, eq 6, we evaluate the integrals in eq 5 for the nth element. The resulting equation is then represented by a local 6×6 matrix. For the left-hand side of eq 5, the matrix representation reads

$$\begin{pmatrix}\psi_n^1\\ \psi_n^{1'}\\ \psi_n^{1''}\\ \psi_n^2\\ \psi_n^{2'}\\ \psi_n^{2''}\end{pmatrix}^T \begin{pmatrix}H_{11}^n & H_{12}^n & H_{13}^n & H_{14}^n & H_{15}^n & H_{16}^n\\ H_{21}^n & H_{22}^n & H_{23}^n & H_{24}^n & H_{25}^n & H_{26}^n\\ H_{31}^n & H_{32}^n & H_{33}^n & H_{34}^n & H_{35}^n & H_{36}^n\\ H_{41}^n & H_{42}^n & H_{43}^n & H_{44}^n & H_{45}^n & H_{46}^n\\ H_{51}^n & H_{52}^n & H_{53}^n & H_{54}^n & H_{55}^n & H_{56}^n\\ H_{61}^n & H_{62}^n & H_{63}^n & H_{64}^n & H_{65}^n & H_{66}^n\end{pmatrix} \begin{pmatrix}\psi_n^1\\ \psi_n^{1'}\\ \psi_n^{1''}\\ \psi_n^2\\ \psi_n^{2'}\\ \psi_n^{2''}\end{pmatrix}$$

The right-hand side of eq 5 can be expressed in a similar matrix form. The matrix elements H_{ij}^n are only function of n, d_h, and λ

These N local matrices are then assembled in such a way that it ensures the continuity of the wave function and its first and its second derivative across elements.[50] The complete problem is now represented by a $(3N + 3) \times (3N + 3)$ matrix equation. In a simplified notation

$$\langle\psi_i|H_{ij}|\psi_j\rangle = \epsilon\langle\psi_i|U_{ij}|\psi_j\rangle \quad (7)$$

The quantity $|\psi_i\rangle$ is the nodal representation of the wave function $\psi(r)$ and its first two derivatives.

So far, we have not included the contribution from region B. The approximation used for this single infinite element is based on the assumption that the potential energy is negligible, and then, it is assumed to be zero. The simplest wave function consistent with this assumption is an exponentially decaying wave function $\psi_B(r) = \psi(r_c)e^{-r}$. This minimal treatment of the infinite element is sufficient to accurately determine the critical parameters of the Yukawa potential. Direct evaluation of eq 5 using $\psi_B(r)$ leads to a simple correction to the (4,4) element of the local matrices corresponding to the Nth element of region A.

Equation 7 is the discrete equivalent of eq 5. Performing a variation on the nodal values ψ_i, we obtain a generalized eigenvalue problem representing the initial Schrödinger equation

$$H_{ij}|\psi_j\rangle = \epsilon U_{ij}|\psi_j\rangle \quad (8)$$

Solution of eq 8 is achieved using standard numerical packages.

The importance of using the infinite element in order to incorporate region B is exemplified in Figure 1. For large λ (compared with the critical value), the inclusion of region B has no effect since the solution is a localized, short-range wave function. At small λ, the solution using the cutoff is necessarily localized, with a small negative ground-state eigenvalue. The use of the infinite element allows the delocalization of the wave function, which, in turn, results in a positive eigenvalue for sufficiently small λ.

III. FSS with FEM

The finite-size scaling method (FSS) is a systematic way to extract the critical behavior of an infinite system from analysis on finite systems. To apply the FSS method to quantum problems that exhibit a critical behavior depending on a parameter λ, we separate the Hamiltonian in the form

$$H = H_0 + V_\lambda \quad (9)$$

where we have isolated the λ-dependent part in the second term, V_λ. We are interested in how the system changes as the value of λ changes. For the Yukawa potential, there is a critical point λ_c that indicates where the bound state becomes degenerate with the continuum. Then, for any $\lambda > \lambda_c$, the system has a bound state with energy E_λ, which becomes zero for $\lambda = \lambda_c$. For $\lambda < \lambda_c$, the solution is delocalized.

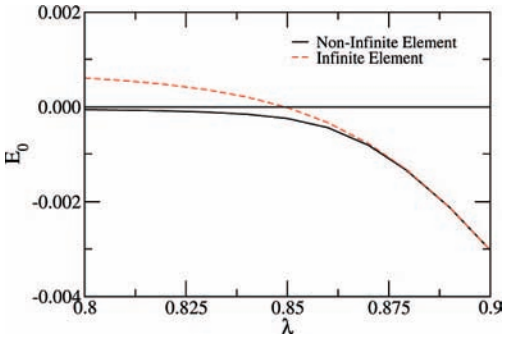

Figure 1. Ground-state energy calculated using a distance cutoff r_c (solid, black line) and including the infinite element for $r > r_c$ (dashed, red line). The calculations were performed using $N = 200$ finite elements.

As in statistical mechanics, there are critical exponents related to the asymptotic behavior of different properties near the critical point. For our study, we define the exponent α for the energy as

$$E_\lambda \approx (\lambda - \lambda_c)^\alpha \tag{10}$$

In previous studies of quantum criticality,[15,16] the wave function is expanded, to order N, in a complete basis set. The order of the expansion is analogous to the system size of the standard FSS method used in statistical mechanics. Thus, increasing the order of the expansion corresponds to an increase in the finite size. It is worth noting at this point that the larger expansions contain the terms included in the smaller expansions.

For the purpose of implementing FSS based on a solution of the Schrödinger equation obtained with FEM, the finite size will now correspond to the number of elements used to construct the global matrix. The solution region is discretized into N elements of length d_h. We have, in principle, two ways to increase the number of elements N for the subsequent solutions needed to implement the FSS scheme. The first involves a constant solution region with a finer discretization (smaller d_h) while increasing N. The second involves a constant element size (d_h) and a larger solution region as N is increased. Both methods were tested, but only the second one produced consistent results. As in the basis set case, the inclusion of the smaller system solutions into the larger solution region is essential for the implementation of FSS.

The wave function inside of the nth element is described by eq 6. The numerical solution of the generalized eigenvalue problem (see above) gives the set of nodal values for the wave function and its first two derivatives. These nodal points are interpolated with the Hermite interpolation polynomials (see eq 6) to produce a continuum solution inside of each element. Then, the average value of any operator, calculated with N finite elements, can be expressed as a sum of all of the contributions from the individual elements (the angular factors are irrelevant for our purpose of FSS)

$$\langle O\rangle^N = \sum_{n=1}^{N} \int_{r_n}^{r_{n+1}} r^2 \psi_n^*(r) O \psi_n(r) \mathrm{d}r + \int_{r_c}^{\infty} r^2 \psi_B^*(r) O \psi_B(r) \mathrm{d}r \tag{11}$$

If the mean value of a λ-dependent operator $\langle O\rangle_\lambda$ is not analytical at $\lambda = \lambda_c$, then we define a critical exponent μ_O with the following relation

$$\langle O\rangle_\lambda \approx (\lambda - \lambda_c)^{\mu_O} \qquad \text{for } \lambda \to \lambda_c^+ \tag{12}$$

where $\lambda \to \lambda_c^+$ represents taking the limit of λ approaching the critical point from larger values of λ. By using FEM, the singularities in the mean values will occur only by using an infinite number of elements and, therefore, a truly infinite solution range. Following the same approach as FSS in statistical mechanics, we assume the existence of a scaling function that relates the mean value of any operator calculated with N elements to its limiting value

$$\langle O\rangle_\lambda^{(N)} \sim \langle O\rangle_\lambda F_O(N|\lambda - \lambda_c|^\nu) \tag{13}$$

with the scaling function F_O being particular for different operators but all having the same unique scaling exponent ν.

To obtain the critical parameters, we define the following function

$$\Delta_O(\lambda; N, N') = \frac{\ln(\langle O\rangle_\lambda^N / \langle O\rangle_\lambda^{N'})}{\ln(N'/N)} \tag{14}$$

At the critical point, the expectation value is related to N as a power law, $\langle O\rangle \sim N^{\mu_O/\nu}$, and eq 14 become independet of N. For the energy operator $O = H$, and using the customary α Greek letter for the corresponding exponent μ_O, we have

$$\Delta_H(\lambda_c; N, N') = \frac{\alpha}{\nu} \tag{15}$$

In order to obtain the critical exponent α from numerical calculations, it is convenient to define a new function[15]

$$\Gamma_\alpha(\lambda, N, N') = \frac{\Delta_H(\lambda; N, N')}{\Delta_H(\lambda; N, N') - \Delta_{\frac{\partial V_\lambda}{\partial \lambda}}(\lambda; N, N')} \tag{16}$$

which, at the critical point, is independent of N and N' and takes the value of α. Namely, for $\lambda = \lambda_c$ and any values of N and N', we have

$$\Gamma_\alpha(\lambda_c, N, N') = \alpha \tag{17}$$

and using eq 15

$$\nu = \frac{\alpha}{\Delta_H(\lambda_c; N, N')} \tag{18}$$

Using three finite elements solutions obtained with a different number of elements (N, N', and N''), we calculate two Γ curves using eq 16. The intersection of the two curves define $\lambda_c^{(N)}$, $\alpha^{(N)}$. Then, $\nu^{(N)}$ is readily calculated from eq 18. The citical values are then obtained from the succesion of values as a function of $1/N$ by performing an extrapolation for $1/N \to 0$.

IV. Results and Discussion

For previous studies of the Yukawa potential, parity effects were observed depending on the basis set used.[16]

However, in this case with the finite element method, there were no observed parity effects. The finite-size scaling equations are valid only as asymptotic expressions, but unique values of λ_c, α, and ν can be obtained as a succession of values as a function of N. The lengths of the elements are set to $d_h = 1.0$ for both $l = 0$ and 1. This choice was done based on the stability of the numerical solutions.

In Figure 2, we show the behavior of the ground-state energy as a function of λ for $l = 0$. We see that as the number of elements increases, the ground-state energy becomes positive at a λ value closer to λ_c. However, an exact solution would require an infinite number of elements. Therefore, the FSS method is necessary in order to determine critical parameters. In Figure 3, the function Γ is plotted for different values of N. As mentioned before, these curves are independent of N at the

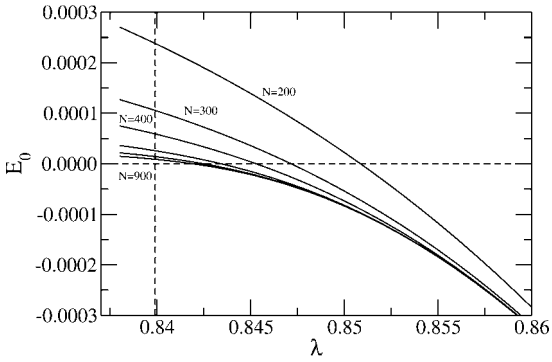

Figure 2. Behavior of the ground-state energy as a function of λ for $N = 200$, 300, 400, 500, 700, and 900. The vertical line shows our best estimation for λ_c.

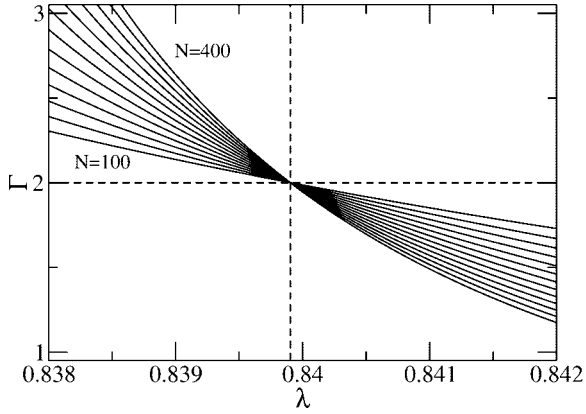

Figure 3. Plot of Γ as a function of λ using N from 100 to 400 in steps of 25. The crossing of the dashed lines indicates the critical values λ_c and α.

critical point. Namely, the intersection of the curves indicates the critical point (λ_c, α).

For each of the values of N, we actually solve the problem three times (N, $N + 1$, and $N + 2$) in order to obtain two Γ curves. The crossing of these two curves defines the pseudocritical parameters $\lambda_c^{(N)}$ and $\alpha^{(N)}$. The exponent $\nu^{(N)}$ is easily obtained from eq 18. In Figure 4, we observe the behavior of the pseudocritical parameters as a function of $1/N$. The three curves monotonically converge to limiting values. Then, by applying the Bulirsch−Stoer algorithm,[51] we are able to obtain the values of λ_c, α, and ν, which are displayed in Figure 4 as a solid circle and summarized in Table 1. The critical parameters λ_c and α are displayed as dashed lines in Figure 3, showing the consistency of our results.

The ground-state energy for $l = 1$ as a function of λ and a different number of finite elements is displayed in Figure 5. Three main features should be noticed. First, for $\lambda > \lambda_c$, the effect of increasing the number of elements is negligible. Second, all of the curves become positives for λ very near the critical point, indicating that the number of elements needed to obtain a good estimation of the critical parameters is smaller than that in the case corresponding to $l = 0$. Third, the curves show a very abrupt transition for λ that is slightly smaller than that for λ_c. This transition is very pronounced and is noticeable even with a smaller number of elements. This behavior is indicative of a first-order transition, characterized by $\alpha = 1$. In Figure 6, we show the behavior of the pseudocritical parameters as a function of $1/N$. As in the case of $l = 0$, the three curves converge monotonicaly to well-defined values and allow for the application of the Bulirsch−Stoer algorithm to extract the critical parameters, which are shown in Table 1.

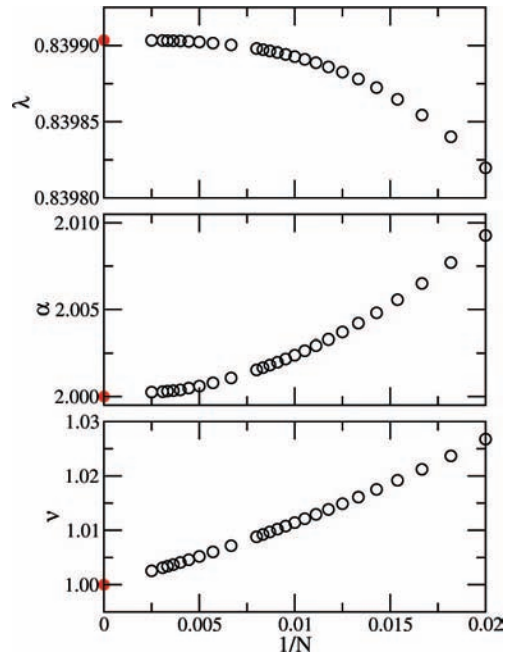

Figure 4. Pseudocritical parameterrs as a function of the inverse of the number of elements. The red dots at $1/N = 0$ are the result of the extrapolation using the Bulirsch−Stoer algorithm.

TABLE 1: Results for Critical Parameters

	this work	ref 15	exact
	$l = 0$		
λ_c	0.839 903 45(5)	0.839 903 9(1)	
α	2.000 2(2)	2.000 00(2)	2
ν	1.002(2)	0.999 9(2)	1
	$l = 1$		
λ_c	4.540 983 18(5)	4.540 980(3)	
α	0.999 9(6)	0.999 9(3)	1
ν	0.500 2(2)	0.501(1)	0.5

We have conventiently summarized our results for the critical parameters for both $l = 0$ and 1 in Table 1. For reference, we include the corresponding values obtained using expansion on the Slater-type basis set, as well as the known exact ciritical exponents.

To check the correctness of our finite-size scaling assumptions, we performed a data collapse calculation of the Yukawa potential as done before in previous studies.[52] In Figure 7, we plot the results corresponding to $l = 0$ (top panel) and 1 (bottom panel), which have been calculated with the critical parameters summarized in Table 1. We see that the curves do indeed collapse into one, which gives strong support for the results of combining the FEM with FSS.

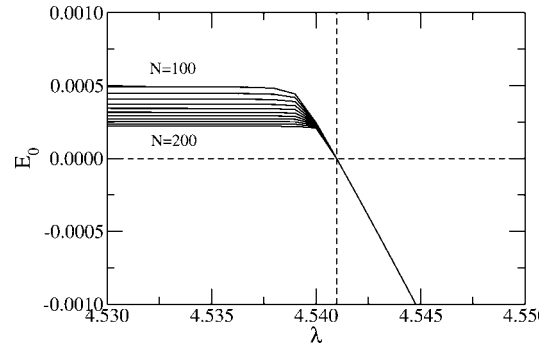

Figure 5. Behavior of the ground-state energy as a function of λ for $l = 1$ with the number of elements from $N = 100$ to 200. The vertical dashed line indicates λ_c.

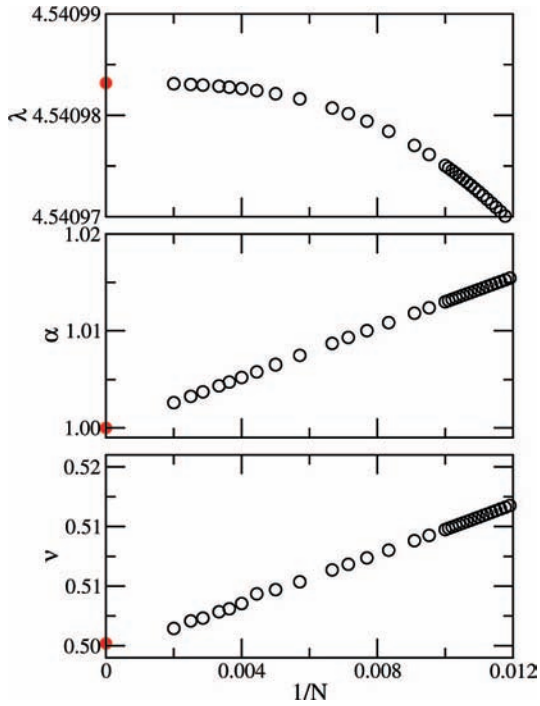

Figure 6. Pseudocritical parameters as a function of the inverse of the number of elements for $l = 1$. The red dots at $1/N = 0$ are the extrapolated critical values.

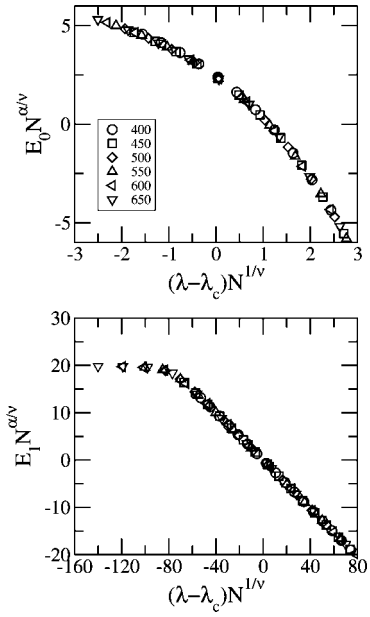

Figure 7. Data collapse for the ground-state energy corresponding to $l = 0$ (top panel) and 1 (bottom panel).

In conclusion, we have performed a finite-size scaling analysis of the short-ranged Yukawa potential with the finite element method. We were able to study the different behavior of the critical parameters for our system. The critical parameters obtained were in excellent agreement with previous reference values. The data collapse results strongly support the assumptions made for the finite-size scaling ansatz with finite elements. This new approach with FSS is simple and easily combined with FEM to produce accurate results.

Acknowledgment. We would like to acknowledge the financial support of the Army Research Office (ARO). We also thank Dr. Rikkert Nap for simplifying the procedure of generating the local matrices needed for FEM.

References and Notes

(1) Yang, C. N.; Lee, T. D. *Phys. Rev.* **1952**, *87*, 404.
(2) Lee, T. D.; Yang, C. N. *Phys. Rev.* **1952**, *87*, 410.
(3) (a) Fisher, M. E. In *Critical Phenomena*, Proceedings of the 51st Enrico Fermi Summer School, Varenna, Italy; Green, M. S., Ed.; Academic Press: New York, 1971. (b) Fisher, M. E.; Barber, M. N. *Phys. Rev. Lett.* **1972**, *28*, 1516.
(4) Widom, B. *Critical Phenomena in Fundamental Problems in Statistical Mechanics*; Cohen, E. G. D., Ed.; Elsevier Publishing Company: New York, 1975.
(5) Barber, M. N., Finite Size Scaling. In *Phase Transitions and Critical Phenomena*; Domb, C., Lebowits, J. L. , Eds.; Academic Press: London, 1983; Vol. 8.
(6) Privman, V. *Finite Size Scaling and Numerical Simulations of Statistical Systems*; World Scientific: Singapore, 1990.
(7) Cardy, J. L. *Finite-Size Scaling*; Elsevier Science Publishers B.V.: New York, 1988.
(8) Nightingale, M. P. *Physica A* **1976**, *83*, 561.
(9) Reynolds, P. J.; Stanley, H. E.; Klein, W. *J. Phys. A* **1978**, *11*, L199.
(10) Reynolds, P. J.; Stanley, H. E.; Klein, W. *Phys. Rev. B* **1980**, *21*, 1223.
(11) Stanley, H. E.; Reynolds, P. J.; Redner, S.; Family, F. Position Space Renormalization Group for Models of Linear Polymers, Branched Polymers and Gels. In *Topics in Current Physics, Vol. 30, Real Space Renormalization,*; Burkhardt, T. W., van Leeuwen, M. J., Eds.; Springer Verlag: Berlin, 1982; Chapter 7.
(12) Neirotti, J. P.; Serra, P.; Kais, S. *Phys. Rev. Lett.* **1997**, *79*, 3142.
(13) Serra, P.; Neirotti, J. P.; Kais, S. *Phys. Rev. Lett.* **1998**, *80*, 5293.
(14) Kais, S.; Neirotti, J. P.; Serra, P. *Int. J. Mass Spectrom.* **1999**, *182/183*, 23.
(15) Serra, P.; Neirotti, J. P.; Kais, S. *Phys. Rev. A* **1998**, *57*, R1481.
(16) Serra, P.; Neirotti, J. P.; Kais, S. *J. Phys. Chem. A* **1998**, *102*, 9518.
(17) Neirotti, J. P.; Serra, P.; Kais, S. *J. Chem. Phys.* **1998**, *108*, 2765.
(18) Shi, Q.; Kais, S. *Mol. Phys.* **2000**, *98*, 1485.
(19) Kais, S.; Shi, Q. *Phys. Rev. A* **2000**, *62*, 60502.
(20) Kais, S.; Serra, P. *Int. Rev. Phys. Chem.* **2000**, *19*, 97.
(21) Kais, S.; Serra, P. *Adv. Chem. Phys.* **2003**, *125*, 1.
(22) Baker, J. D.; Freund, D. E.; Hill, R. N.; Morgan, J. D. *Phys. Rev. A* **1990**, *41*, 1247.
(23) Ivanov, I. A. *Phys. Rev. A* **1995**, *51*, 1080.
(24) Serra, P.; Kais, S. *Chem. Phys. Lett.* **2003**, *372*, 205.
(25) Ferron, A.; Serra, P.; Kais, S. *J. Chem. Phys.* **2004**, *120*, 8412.
(26) Shi, Q.; Kais, S. *Mol. Phys.* **2000**, *98*, 1485.
(27) Shi, Q.; Kais, S. *Int. J. Quantum Chem.* **2001**, *85*, 307.
(28) Shi, Q.; Kais, S. *J. Chem. Phys.* **2004**, *121*, 5611.
(29) Serra, P.; Kais, S.; Moiseyev, N. *Phys. Rev. A* **2001**, *64*, 062502.
(30) Moy, W; Serra, P.; Kais, S. *Mol. Phys*. **2008**, *106*, 203.
(31) Hrenikoff, A. *J. Appl. Mech.* **1941**, *8*, 169.
(32) Courant, R. *Bull. Am. Math. Soc.* **1943**, *49*, 1.
(33) Argyris, J. H.; Kelsey, S. *Energy Theorems and Structural Analysis*; Butterworth Scientific Publications: London, 1960.
(34) Turner, M.; Clough, R. W.; Martin, H. H.; Topp, L. *J. Aeronaut. Sci.* **1956**, *23*, 805.
(35) Owen, D. R. J.; Hinton, E. *Simple Guide for Finite Elements*; Pinepridge Press: Swansea, U.K., 981.
(36) Duff, M.; Rabitz, H.; Askar, A.; Cakmak, A.; Ablowitz, M. *J. Chem. Phys.* **1980**, *72*, 1543.
(37) Flores, J. R.; Clementi, E.; Sonnad, V. *Chem. Phys. Lett.* **1989**, *163*, 198.
(38) Ram-Mohan, L. R.; Saigal, S.; Dossa, D.; Shertzer, J. *Comp. Phys* **1990**, *Jan/Feb*, 50.
(39) Braun, M.; Schweizer, W.; Herold, H. *Phys. Rev. A* **1993**, *48*, 1916.
(40) Ackermann, J. *Phys. Rev. A* **1995**, *52*, 1968.
(41) Zheng, W.; Ying, L.; Ding, P. *Appl. Math. Comput.* **2004**, *153*, 685.
(42) Heinemann, D.; Fricke, B.; Kolb, D. *Phys. Rev. A* **1988**, *38*, 4994.
(43) Braun, M.; Elster, H.; Schweizer, W. *Phys. Rev. A* **1998**, *57*, 3739.
(44) Sundholm, D.; Olsen, J. *J. Chem. Phys.* **1991**, *94*, 5051.
(45) Yu, H.; Bandrauk, A.; Sonnad, V. *J. Math. Chem.* **1994**, *15*, 273.
(46) Yu, H.; Bandrauk, A.; Sonnad, V. *J. Math. Chem.* **1994**, *15*, 287.
(47) Pepper, D. W.; Heinrich, J. C. *The Finite Element Method*; Taylor & Francis: New York, 2006.
(48) Reddy, J. N. *An Introduction to the Finite Element Method*; McGraw-Hill: St. Louis, MO, 1993.
(49) Ram-Mohan, L. R. *Finite Element and Boundary Element Applications in Quantum Mechanics*; Oxford University Press: New York, 2002.
(50) Schweizer, W. *Numerical Quantum Dynamics*; Kluwer Academic Publishers: Boston, MA, 2001.
(51) Monroe, J. L. *Phys. Rev. E* **2002**, *65*, 066116.
(52) Serra, P.; Kais, S. *Chem. Phys. Lett.* **2000**, *319*, 273.

JP800346Z